



HAL
open science

Spectroscopic identification of active centers and reaction pathways on MoS₂ catalyst for H₂ production via water-gas shift reaction

Weitao Zhao, Françoise Maugé, Jianjun Chen, Laetitia Oliviero

► To cite this version:

Weitao Zhao, Françoise Maugé, Jianjun Chen, Laetitia Oliviero. Spectroscopic identification of active centers and reaction pathways on MoS₂ catalyst for H₂ production via water-gas shift reaction. Chemical Engineering Journal, 2023, 455, pp.140575. 10.1016/j.cej.2022.140575 . hal-04300293

HAL Id: hal-04300293

<https://hal.science/hal-04300293>

Submitted on 22 Nov 2023

HAL is a multi-disciplinary open access archive for the deposit and dissemination of scientific research documents, whether they are published or not. The documents may come from teaching and research institutions in France or abroad, or from public or private research centers.

L'archive ouverte pluridisciplinaire **HAL**, est destinée au dépôt et à la diffusion de documents scientifiques de niveau recherche, publiés ou non, émanant des établissements d'enseignement et de recherche français ou étrangers, des laboratoires publics ou privés.

1 Spectroscopic identification of active centers and
2 reaction pathways on MoS₂ catalyst for H₂ production
3 via water-gas shift reaction
4

5 *Weitao Zhao¹, Françoise Maugé¹, Jianjun Chen² and Laetitia Oliviero^{1*}*

6 ¹ Normandie Université, ENSICAEN, UNICAEN, CNRS, LCS, 14000 Caen, France

7 ² School of Environment, Tsinghua University, Beijing 100084, China

8 KEYWORDS: S/O exchange • sulfur vacancy • MoS₂ edges • reaction mechanism • structure-activity
9 relationships • deactivation.

10 ABSTRACT

11 In previous reports, it was proposed that the oxygen-substituted Mo(S_xO_y)_{zc} site formed *in situ* by water
12 is active center for water-gas shift reaction catalyzed by MoS₂. However, water is also hypothesized to
13 be the driving force for sulfide catalyst deactivation. This irreconcilable dispute stems from the limited
14 understanding about the reaction mechanism and the lack of relevant *in situ* or/and *operando*
15 characterization. In this work, the different reactivity of the two preferentially exposed MoS₂ edge sites,
16 M-edge and S-edge sites, with CO and H₂O is revealed by means of *in situ* CO adsorption followed by
17 IR spectroscopy. Isotopic reactants (¹³CO/¹²CO ; H₂¹⁸O) were used to account for the origin of the
18 formed products and catalyst surface modification. In particular, upon H₂O feed, S/O exchange occurs

19 on M-edge leading to $\text{Mo}(\text{S}_x\text{O}_y)_{zc}$ sites that are not reactive towards subsequent CO feed in
20 contradiction with a redox mechanism in which the catalyst surface is first exchanged by H_2O and then
21 reduced by CO. Moreover, the M-edge sites hardly give vacancy under CO treatment. Conversely, the
22 S-edge sites are much less prone to S/O exchange upon H_2O feed but are sensitive to CO to form
23 vacancies and release COS. In addition, IR *operando* studies are in accordance with a formate pathway
24 and a novel redox mechanism via COS formation. This insight into the catalytic active sites under
25 reaction conditions allows to identify the M-edge sites as the ones leading to the deactivation of the
26 catalyst and the S-edge sites as the redox active sites. Thus, the work gives the direction for the rational
27 design of high-performance and stable sulfide catalysts for reactions involving H_2O dissociation and CO
28 conversion.

29

30 1. Introduction

31 Molybdenum-based sulfide catalysts find extensive applications in various catalytic processes such as
32 hydrodesulfurization, CO₂ hydrogenation as well as hydrogen production by water electrolysis and the
33 water gas shift (WGS) reaction [1-5]. The catalytic activity for MoS₂ has been reported to mainly arises
34 from the coordinatively unsaturated sites located along the edge of MoS₂ slabs rather than the saturated-
35 coordination sites in basal plane [6, 7]. However, with the development of characterization technology,
36 the understanding of active sites has also changed. Recently, in-plane sulfur atoms can be substituted by
37 oxygen atoms doped into the MoS₂ [8-10], and this formed MoS_{2-x}O_x sites can also act as active sites for
38 hydrogen evolution reaction (HER) due to its good electrical conductivity [11]. Similarly, the
39 importance of MoS_{2-x}O_x site formed *in situ* as a result of hydrolysis has been recognized momentarily
40 for WGS reaction, and hitherto it has been proposed as an active center reacting with CO to release CO₂
41 [12, 13]. However, due to the lack of the sophisticated *in situ* characterization techniques on supported
42 MoS₂ catalysts, this hypothesis involving MoS_{2-x}O_x site as WGS active center is not yet fully
43 experimentally verified and thus understanding the actual surface reaction at surface of MoS₂ should be
44 significant deepened.

45 Another ambiguous issue is the comparative study of edge sites for their catalytic reactivity.
46 Theoretical and experimental studies reveal the existence of two types of low-index edge terminations
47 with different coordination environment over MoS₂ slab, i.e. the (10 $\bar{1}$ 0) M edge and the ($\bar{1}$ 010) S edge
48 [4, 14-17]. Such different coordination structures in M- and S-edge sites determine that they would have
49 different reactivity. This point has been demonstrated in thiophene HDS reaction for which the intrinsic
50 activity of S-edge sites is higher than that of M-edge sites [4]. However, for HER and WGS reaction,
51 the comparative study of the two edge sites activity is experimentally rare, and most of the studies
52 mainly focus on theoretical calculation. For instance, comparing the hydrogen bond energy, hydrogen
53 evolution on MoS₂ is expected to occur predominantly at the M-edge ($\Delta G_{\text{H}} = 0.08$ eV) rather than S-

54 edge ($\Delta G_H = 0.18$ eV) [18]. With respect to WGS reaction, there have been disagreements on mechanism
55 over MoS₂ catalyst. Some researchers attribute formate species to spectator (formed by a side reaction
56 between CO₂ and H) and claim that both M- and S-edge sites follow a redox mechanism of successive
57 surface oxidation by H₂O and reduction by CO [19, 20]; others correlate the formate to a favorable
58 intermediate (formed via CO reaction with OH) on both edges of MoS₂ and thus propose a double
59 mechanism through redox and associative paths [21]. However, even the widely accepted redox
60 mechanism that supports the MoS_{2-x}O_x site as active center does not allow to understand why sulfide
61 catalysts would exhibit poor stability under H₂S-free condition, which is often interpreted as poor anti-
62 oxidation capability for the formation of oxy-sulfide phase during the WGS reaction. On the contrary,
63 the catalytic performance and stability would be significantly enhanced in H₂S-containing atmosphere
64 [22, 23]. These highly divergent results indicate that redox mechanism is not well understood, especially
65 for the role of MoS_{2-x}O_x sites. Furthermore, the role of the support also requires special consideration
66 [24]. On one hand, CO adsorbed on sulfide sites could spill over to the support [25], implying that the
67 support could be involved in catalytic reaction whereas only sulfide phase is considered in DFT
68 calculation; on the other hand, the interaction between the sulfide phase and the support results in
69 varying the proportion of M-edge to S-edge sites [26], also affecting the catalytic activity [22].
70 Therefore, a direct observation of the catalytic performance of specific sites is required to get insight
71 into the reactivity of M-/S-edge site.

72 The crucial issue in the surface reaction investigation on MoS₂ is how to readily identify and quantify
73 each type of edge sites. In general, visual observation of morphology can be directly achieved by
74 electron microscopy to qualitatively distinguish the two exposed edges. However, active metal
75 dispersion as measured by microscopy is limited by statistical information. Fourier transform infrared
76 (FTIR) spectroscopy coupled with probe molecules appears to be a powerful method by monitoring with
77 the sufficient sensitivity the probe-surface interaction. In particular, all aspects of the catalyst system in

78 terms of the sulfide/support surface, titration of active edge sites, and electron transfer can be probed by
79 CO adsorption at liquid nitrogen temperature followed by IR spectroscopy (CO/IR) [27-30]. Meanwhile,
80 CO can also represent the realistic active site information being a reactant in WGS reaction.

81 In this work, two kinds of MoS₂/Al₂O₃ catalysts have been prepared with/or without citric acid
82 through wetness impregnation method in order to obtain two morphologies of MoS₂ slabs with different
83 proportion of M-edge to S-edge sites [4]. Next, the reactivity of each type of edge sites towards H₂O
84 and/or CO is studied using CO/IR spectroscopy technique. Then, the stepwise WGS surface reaction is
85 carried out to elucidate the mechanism routes. Finally, *operando* study coupling IR analysis of the
86 catalyst surface and IR/GC analysis of the gas phase confirms the routes through *operando*
87 identification of relevant long-lived intermediates. This work is the first to explore the effect of H₂O and
88 CO on both M-edge and S-edge sites, allowing to identify the real active center of sulfide catalyst and to
89 reveal the mechanism of WGS reaction. More importantly, understanding the reactivity of the M/S-edge
90 sites with H₂O and CO also contributes to the design of sulfide catalysts for other reactions involving
91 H₂O dissociation and CO conversion.

92

93 **2. Experimental Section**

94 **2.1. Catalyst preparation**

95 Mo/Al₂O₃ catalyst was prepared by wetness impregnation method using ammonium heptamolybdate
96 tetrahydrated salt as molybdenum precursor ((NH₄)₆Mo₇O₂₄·4H₂O, MERCK). The supports, γ-Al₂O₃
97 (245 m²/g, Sasol), were crushed and sieved into 0.2-0.5 μm fraction and then pre-calcined at 773K
98 during 4h. The loading of Mo was targeted at a sub monolayer with 3 atoms Mo/nm². In addition,
99 Mo(CA=2)/Al₂O₃ catalyst was prepared by same method but with citric acid (CA, C₆H₈O₇·H₂O,
100 PROLABO) as a chelating agent and the molar ratio of citric acid to Mo was kept at 2. After
101 impregnation, the catalysts were left for maturation at ambient for 2h and then dried at 383K (1K/min)

102 during 16h. Note that the catalysts were not calcined in order to keep the chelating agent in its initial
103 form. Mo/SiO₂ catalyst was prepared with same method than Mo/Al₂O₃ on SiO₂ (506 m²/g, Merk).

104 **2.2. Catalyst sulfidation**

105 Catalyst sulfidation were performed *in situ* in a quartz glass IR cell. Sample was firstly grounded and
106 pressed into a self-supporting pellet of ~20 mg and area of 2 cm² (precisely weighted). The pellet was
107 then introduced into the glass cell and the cell was evacuated to $\sim 1.0 \times 10^{-6}$ torr to remove the air and
108 physisorbed water. Afterward, the pellet was activated at atmospheric pressure at 723K in a flow of 30
109 ml/min 10% H₂S/H₂. At the end of activation at 723K for 2h, the IR cell was flushed under Ar flow,
110 then evacuated during 1h at 723K and finally cooled down to room temperature under vacuum.

111 **2.3. Low-temperature CO adsorption followed by IR spectroscopy (CO/IR)**

112 After sulfidation, the pressure in the cell is around $\sim 1.0 \times 10^{-6}$ torr. Then the pellet was cooled down
113 by liquid nitrogen to 100K for CO adsorption. Small calibrated doses of CO were introduced in the IR
114 cell up to an equilibrium pressure of 133 Pa. IR spectra of adsorbed CO were recorded with a Nicolet
115 iS50 FTIR spectrometer equipped with a MCT detector with 256 scans and a resolution of 4 cm⁻¹. For
116 comparison, all the spectra presented were normalized to a sulfided catalyst pellet of 5 mg.cm⁻². The SI
117 give the procedure for treatment after the sulfidation (SI1). The spectra treatment and subsequent
118 calculation are also described in SI2.

119 **2.4. Activity test**

120 Before WGS reaction test, the as prepared catalyst was sulfided at 723K (3K/min) and 0.1MPa for 2h
121 under a 30 ml/min flow of 10% H₂S/H₂. Then WGS reaction was carried out in a glass differential
122 reactor under 0.5% CO and 1% H₂O in Ar balance with GHSV~ 9000 h⁻¹ at 573K and 0.1MPa. The
123 vapor of water was introduced into the system using a saturator with Ar as carrier gas. The water vapor
124 pressure was controlled through a temperature tank set at 17.6°C (20 mbar). The pipelines were heated
125 at 50°C to avoid water condensation. The outlet gas was analyzed by Varian 450 gas chromatograph

126 equipped with a PoraPlot Q column (Varian, 25 m, 0.53 mm, 20 μm) and thermal conductivity (TCD)
127 detector. The catalytic activity was expressed by the conversion of CO. Stepwise test experiments were
128 also performed in glass differential reactor under flow of pure CO or pure H₂O flow (completed by Ar).

129 **2.5. Operando IR/GC experiment**

130 The operando experiments have been performed in a Nicolet 6700 FTIR spectrometer equipped with a
131 specific IR-reactor cell, named IR “sandwich” cell. IR spectra of catalysts were directly recorded by
132 FTIR spectrometer equipped with a MCT detector using 64 scans and a resolution of 4 cm^{-1} .
133 Downstream the IR-reactor cell, the exhaust gases were analyzed simultaneously using an online IR-gas
134 cell and a GC equipped with TCD detector. Catalyst sulfidation were performed *in situ* in the IR-reactor
135 cell reactor. Sample was firstly grounded and pressed into a self-supporting pellet of ~ 15 mg and area of
136 2 cm^2 . The pellet was then installed into the IR-reactor cell. Catalyst sulfidation were performed *in situ*
137 at atmospheric pressure under a flow of 30 ml/min 10% H₂S/H₂ at 723K. Finally, the reactor was cooled
138 down to 573K under pure Ar flow. Afterwards, WGS reaction was carried out under a 10 ml/min feed
139 flow of 0.5% CO and 1% H₂O in Ar balance.

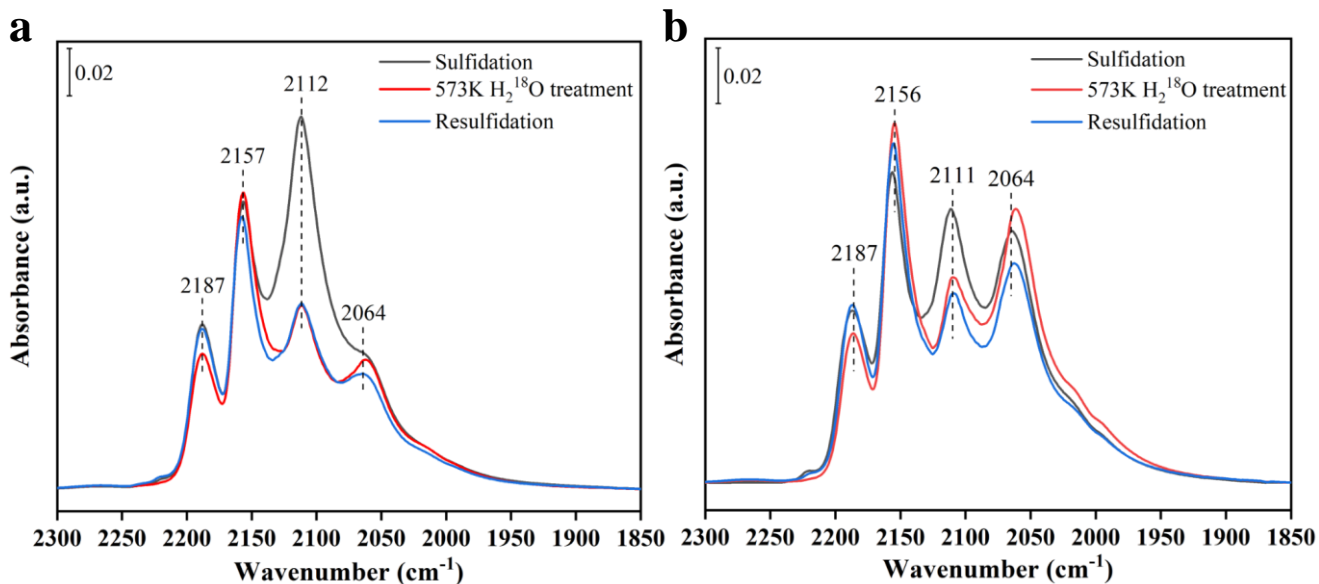
140 **3. Results and Discussion**

141 **3.1. S-edge sites of MoS₂/Al₂O₃ catalysts are not sensitive to water treatment**

142 The reactivity with water of M-edge and S-edge sites of MoS₂ catalysts were evaluated on sulfided
143 Mo/Al₂O₃ and Mo(CA=2)/Al₂O₃ catalysts. CO adsorption (SI1) and HAADF-STEM study [31] have
144 previously demonstrated that the introduction of CA in the impregnation solution leads to higher S-/M-
145 edge ratio with a small decrease in total edge sites (reference J phys chem C jianjun to add). Then, the
146 catalysts were characterized by CO/IR at around 100 K without any air contact after (i) in-situ
147 sulfidation at 723 K, (ii) subsequent treatment under pure H₂¹⁸O vapor at 573 K and (iii) subsequent
148 treatment under 10% H₂S/H₂ at 723K i. e. resulfidation (Figure 1).

149 For both Mo/Al₂O₃ and Mo(CA=2)/Al₂O₃ catalysts, the CO uptake on M-edge sites (band at ~2112
150 cm⁻¹) decreases significantly after water treatment. This is in agreement with previous study and
151 ascribed to an exchange reaction of sulfur-oxygen on the M-edge, making the oxygen-substituted MoS₂
152 sites unfavorable for CO adsorption [32]. Figure 1a and b show that this S/O exchange on M-edge sites
153 is not reversible under 10% H₂S/H₂ treatment indicating the good stability of the formed Mo(S_xO_y)_{zc}
154 sites. This notation is chosen to indicate some O in the coordination environment of Mo edge site
155 without indication of the coordination number nor the proportion of S/O exchange.

156 On Mo/Al₂O₃, the intensity of the ν(CO/S-edge) band at 2064 cm⁻¹ appears unaffected by water
157 treatment whereas an increase of the CO/S-edge band area is observed with a downward shift on
158 Mo(CA=2)/Al₂O₃. Moreover, the water effect on S-edge of Mo(CA=2)/Al₂O₃ catalyst is reversible after
159 the 10% H₂S/H₂ treatment and thus seems to be similar to those observed when sulfur vacancies are
160 created during hydrogen post-treatment (SI2). The creation of vacancies could be related to H₂
161 production during the treatment with H₂O of Mo(CA=2)/Al₂O₃. The surface IR spectrum reveals that
162 carbonaceous residues are present after sulfidation of the catalyst prepared with CA, resulting in bands
163 ranging from 1700 to 1400 cm⁻¹ (SI3 a). After H₂¹⁸O treatment at 573K, discernable changes in the
164 complex signal of the carbonaceous residues are observed. Interestingly, carbon dioxide labeled by
165 isotope ¹⁸O is formed in the gas phase (SI3 b). Thus, H₂¹⁸O is reduced by the residual carbonaceous
166 species and as a consequence, the formation of carbon dioxide should be accompanied by the formation
167 of H₂ (undetectable on IR spectra). Specific formation of H₂ upon H₂O feed on this catalyst will be
168 further confirmed in the stepwise tests described later on.



169

170 **Figure 1. Investigation of the effect of water (H_2^{18}O) treatment on M-edge and S-edge sites.** IR
 171 spectra of CO adsorption at 133 Pa equilibrium on sulfided $\text{Mo}/\text{Al}_2\text{O}_3$ (a) and $\text{Mo}(\text{CA}=2)/\text{Al}_2\text{O}_3$ (b)
 172 catalysts after sulfidation, water treatment (H_2^{18}O , 600 Pa and 573K) and subsequent resulfidation.

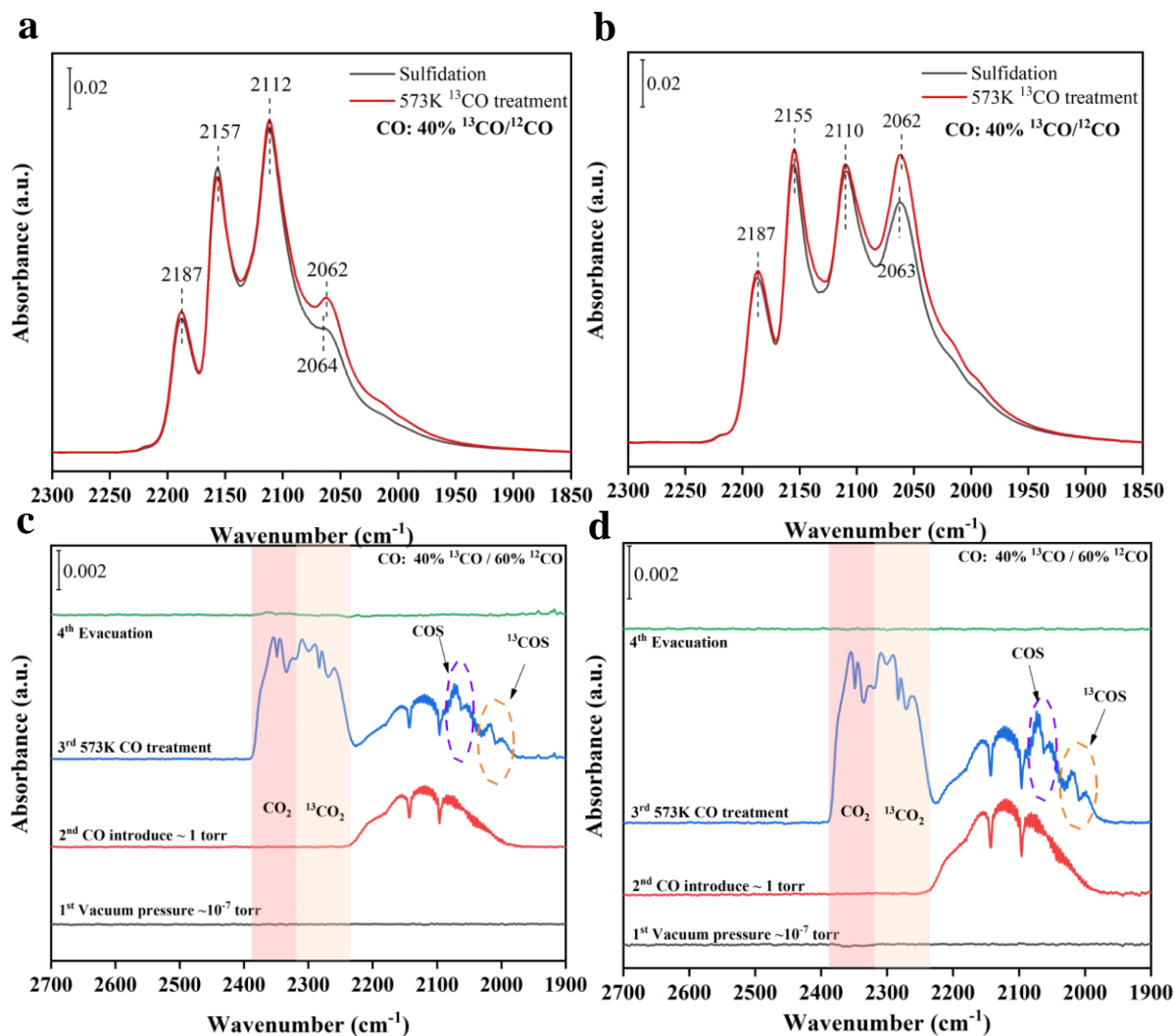
173 Finally, on $\text{Mo}(\text{CA}=2)/\text{Al}_2\text{O}_3$, the intensity of the $\nu(\text{CO}/\text{S-edge})$ band after the resulfidation treatment
 174 is lower than that after the initial sulfidation. In parallel, it has been verified that in absence of water
 175 treatment, resulfidation does not affect the amount of detected S-edge sites (SI4 a). Thus, water
 176 treatment also leads to some irreversible changes of S-edge sites that could be ascribed to some S/O
 177 exchanges during water treatment, in the same way as for the M-edge.

178 In conclusion, two features can occur during water treatment whose extent depend on the sulfide slab
 179 edges: (i) S/O exchange that occurs more easily on M-edge site than on S-edge. (ii) sulfur vacancies
 180 creation that occurs only on S-edge and only on catalyst presenting carbonaceous residues.

181 3.2. S-edge sites of $\text{MoS}_2/\text{Al}_2\text{O}_3$ catalysts form vacancy upon CO treatment

182 The effect of CO treatment (40% $^{13}\text{CO}/60\%^{12}\text{CO}$ at 573K) on edge sites of sulfided catalysts was
 183 probed by CO/IR (^{12}CO at 100K) with a similar strategy than for water treatment. After $\text{Mo}/\text{Al}_2\text{O}_3$ and
 184 $\text{Mo}(\text{CA}=2)/\text{Al}_2\text{O}_3$ catalysts were treated with $^{13}\text{CO}/^{12}\text{CO}$ at 573K, the CO uptake on the S-edge

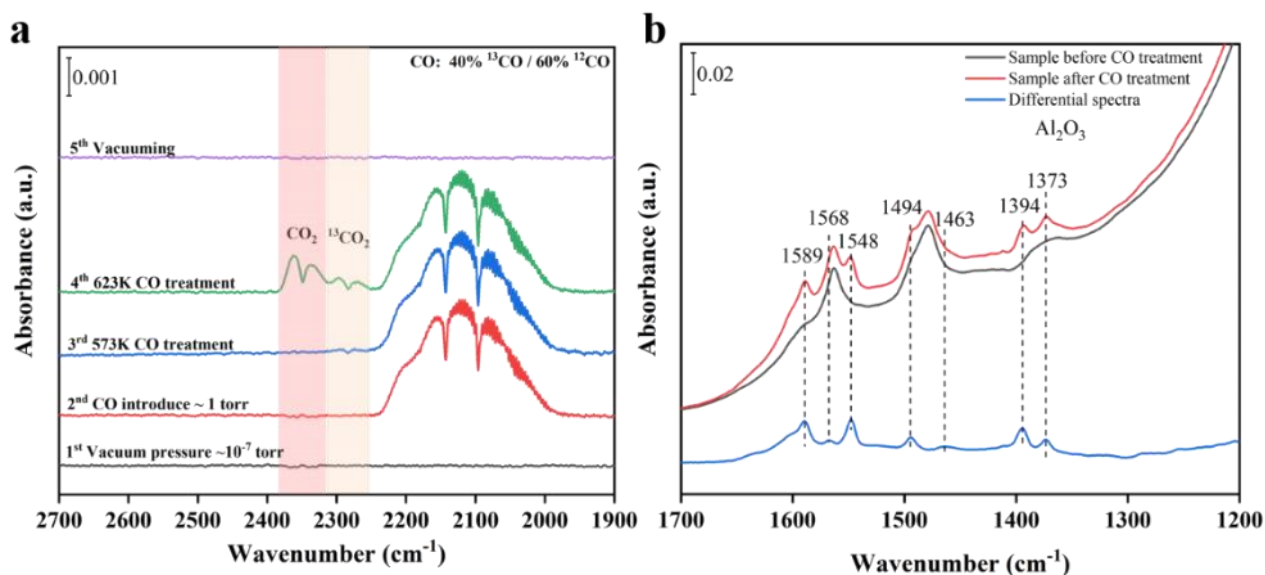
185 increases significantly, while the CO adsorption at the M-edge is almost unchanged (Figure 2, Table 1).
 186 Moreover, the $\nu(\text{CO/S-edge})$ frequency undergoes a slight shift towards lower wavenumber after CO
 187 treatment in accordance with the formation of sulfur vacancy. In addition, resulfidation after CO
 188 treatment was carried out on Mo(CA=2)/Al₂O₃ and the spectrum of CO adsorption (SI6 b) clearly show
 189 that the initial edge state is totally recovered.



190

191 **Figure 2. Investigation of the effect of CO treatment on M-edge and S-edge sites.** a, b, IR spectra of
 192 CO adsorption at 133 Pa equilibrium before and after CO treatment on sulfided Mo/Al₂O₃ catalyst (a)
 193 and Mo(CA=2)/Al₂O₃ catalyst (b). c, d, In-situ IR spectra of gas phase recorded during CO treatment on
 194 sulfided Mo/Al₂O₃ catalyst (c) and Mo(CA=2)/Al₂O₃ catalyst (d).

195 The IR spectra recorded during the CO treatment show the formation of $^{13}\text{COS}/^{12}\text{COS}$ in the gas
 196 phase (Figure 2c and d). These results evidence that CO treatment leads to sulfur vacancy creation
 197 through oxidation of CO into COS. Figure 2a and b points out that S-edge site is more reactive towards
 198 CO treatment than M-edge site. Interestingly, the signal of carbon dioxide was also clearly detected in
 199 gas phase during CO treatment. This could be ascribed to COS hydrolysis on hydroxyl group of support,
 200 or direct reaction of CO with OH group of the support. In order to check the direct reaction between CO
 201 and OH groups, CO treatment was conducted on pure alumina (Figure 3).



202

203 **Figure 3. CO treatment on pure Al_2O_3 .** **a**, *In-situ* IR spectra of gas phase recorded during CO
 204 treatment on Al_2O_3 . **b**, IR spectra of Al_2O_3 recorded before and after CO treatment (CO treatment: 133
 205 Pa 40% $^{13}\text{CO}/60\%^{12}\text{CO}$, 623K/2h).

206 The starting temperature of CO_2 formation on pure Al_2O_3 is 623K, i.e. a higher temperature than on
 207 $\text{Mo}/\text{Al}_2\text{O}_3$. Thus, OH groups of alumina are not active on their own at 573K. However, we cannot
 208 exclude that the presence of sulfide phase enhances the reactivity of CO with OH groups through
 209 adsorbing and/or activating CO on sulfide site and subsequently spilling it over to the support.
 210 Moreover, comparing the IR spectra of Al_2O_3 before and after CO treatment at 623K, it can be found

211 that a small amount of formate species (1589, 1394 and 1373 cm^{-1}) and carbonate species (1548 and
 212 1494 cm^{-1}) was accumulated on the surface of Al_2O_3 . Formate are also observed after CO treatment at
 213 573K on $\text{Mo}/\text{Al}_2\text{O}_3$ (SI5). However, as described above, formate species could be involved in CO_2
 214 production as active species or be only present as spectator ones. To check this point, the stability of
 215 formate species was studied. As shown in Figure S6, formate species on $\text{Mo}/\text{Al}_2\text{O}_3$ decompose into CO_2
 216 starting from 573 K. These results show that both the sulfide sites and OH groups are involved in the
 217 indirect or direct CO_2 formation on $\text{Mo}/\text{Al}_2\text{O}_3$.

218

219 **Table 1:** Concentration of edge sites on $\text{Mo}/\text{Al}_2\text{O}_3$ and $\text{Mo}(\text{CA}=2)/\text{Al}_2\text{O}_3$ catalysts after sulfidation and
 220 CO treatment detected by CO/IR spectra.

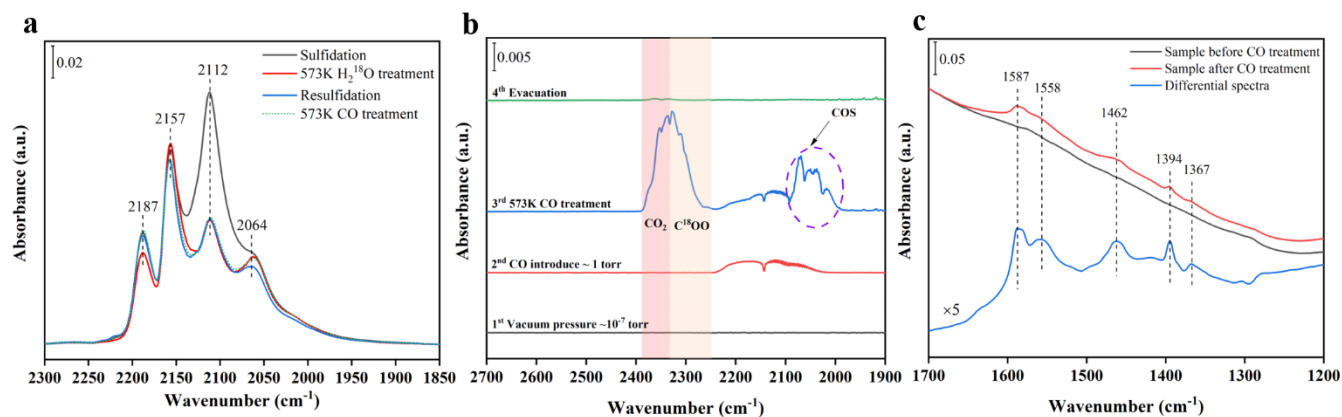
Catalyst	edge	Sulfidation		573K CO	
		$\nu(\text{CO})$ (cm^{-1})	n ($\mu\text{mol g}^{-1}$)	$\nu(\text{CO})$ (cm^{-1})	n ($\mu\text{mol g}^{-1}$)
$\text{Mo}/\text{Al}_2\text{O}_3$	M	2112	59	2112	60
	S	2064	19	2062	25
$\text{Mo}(\text{CA}=2)/\text{Al}_2\text{O}_3$	M	2110	38	2110	39
	S	2063	31	2062	37

221

222 3.3. S/O exchanged sites are not involved in the redox pathway of WGS on $\text{MoS}_2/\text{Al}_2\text{O}_3$ 223 catalysts

224 As mentioned above, because the M-edge site is prone to the S/O exchange reaction, it is most likely
 225 to follow the conventional redox route, with the $\text{Mo}(\text{S}_x\text{O}_y)_{\text{zc}}$ site as the active center. In order to examine
 226 the reactivity of $\text{Mo}(\text{S}_x\text{O}_y)_{\text{zc}}$ sites toward CO, CO/IR was performed stepwise after successive H_2O
 227 treatment, resulfidation and CO treatment at 573 K on sulfided $\text{Mo}/\text{Al}_2\text{O}_3$ catalyst. As shown in Figure

228 4a, the water treatment leads to S-O exchange reaction mainly at M-edge and formation of the
 229 $\text{Mo}(\text{S}_x\text{O}_y)_{z_c}$ sites. Following H_2O treatment, we have seen that the $\text{Mo}(\text{S}_x\text{O}_y)_{z_c}$ on M-edge after
 230 resulfidation is not modified, but also subsequent CO treatment show no effect on the CO adsorption on
 231 M-edge site. In addition, the direct CO treatment after water treatment was also performed on sulfided
 232 $\text{Mo}/\text{Al}_2\text{O}_3$ catalyst (SI7) and the CO uptake of M-edge after $\text{H}_2\text{O} + \text{CO} +$ resulfidation is the same as
 233 that obtained after water treatment, indicating that no $\text{Mo}(\text{S}_x\text{O}_y)_{z_c}$ site is reduced by CO. Thus, the
 234 formation of oxygen vacancy by CO on $\text{Mo}(\text{S}_x\text{O}_y)_{z_c}$ sites of M-edge can be discarded. Note that the CO
 235 uptake on the S-edge increases slightly after CO treatment, this could be attributed to the reaction
 236 between CO and MoS_2 site to create sulfur vacancy, as evidenced by the gas phase analysis which
 237 reveals the formation of COS (Figure 4b). As previously, CO_2 ($\text{C}^{16}\text{O}_2 + \text{C}^{18}\text{O}^{16}\text{O}$) is also detected (Figure
 238 4b) but the CO_2/CO ratio is greater than for CO treatment performed directly after sulfidation (Figure
 239 2). This could be ascribed to the enhanced COS hydrolysis and CO reactivity with hydroxyl group on
 240 the hydrated support. Indeed, formate species (Figure 4c) are observed on the catalyst surface.
 241



242
 243 **Figure 4. Subsequent CO treatment on water treated sulfided $\text{Mo}/\text{Al}_2\text{O}_3$ catalyst.** a, CO/IR spectra
 244 recorded at 133 Pa equilibrium after sulfidation, water treatment, resulfidation, and subsequent CO
 245 treatment. b, *in situ* IR spectra of gas phase recorded during CO treatment. c, IR spectra of catalyst
 246 surface recorded before and after CO treatment in a.

247

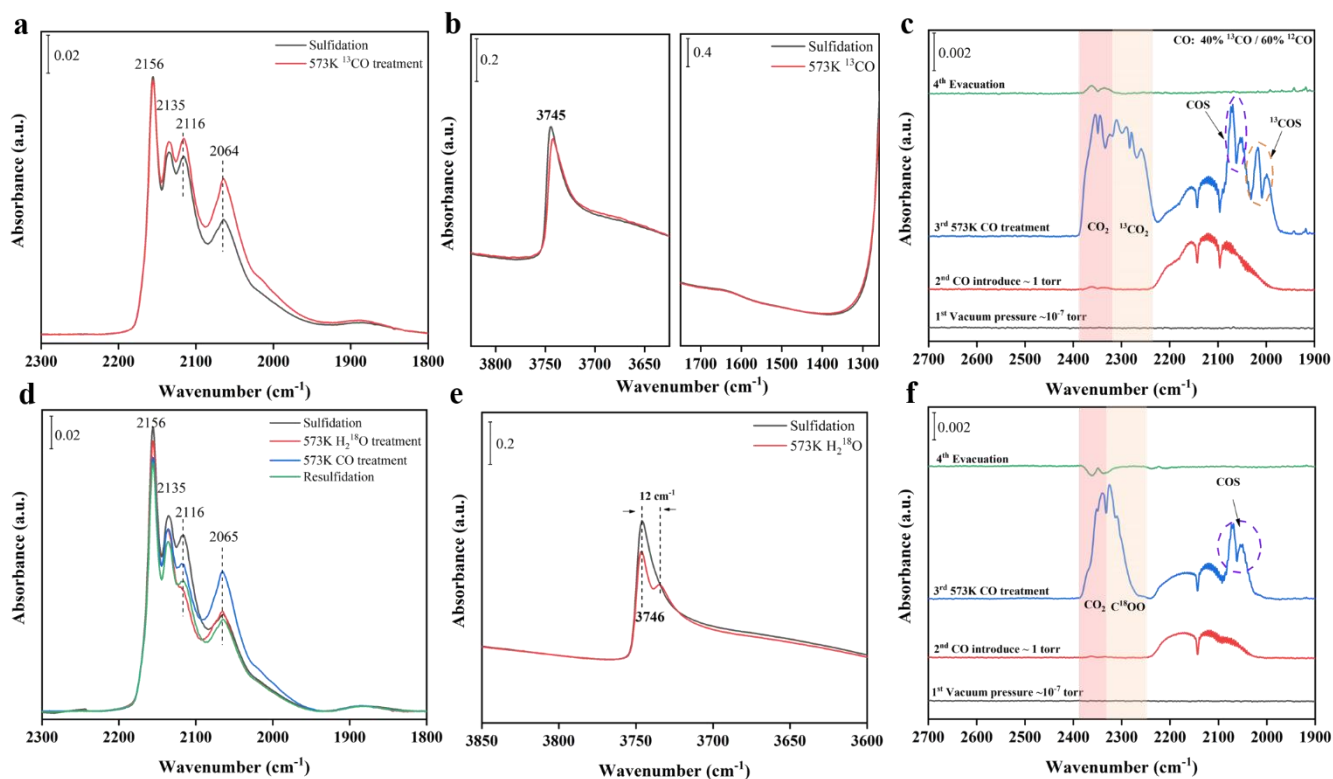
248 **3.4. The support also has a role in WGS pathway**

249 In order to discriminate between the two possible pathways to form CO₂ from CO, i.e. COS
250 hydrolysis pathway or formate pathway, similar study has been performed on Mo/SiO₂. Indeed, on
251 Mo/SiO₂, no formate is expected to be formed on the support. Meanwhile, its sulfide phase is known to
252 have preferentially S-edge sites exposed as confirmed by Figure 5a [26]. From the spectrum after
253 sulfidation, the concentration of sites is calculated to be 17 μmol.g⁻¹ for S-edge and 33 μmol.g⁻¹ for M-
254 edge.

255 As shown in Figure 5a and c, CO (40%¹³CO/60%¹²CO) treatment of sulfided Mo/SiO₂ leads to the
256 formation of vacancies mainly on S-edge along with the formation of carbonyl sulfide and carbon
257 dioxide. This is consistent with results on Al₂O₃-supported Mo catalysts. However, on Mo/SiO₂, the
258 carbon dioxide should be formed through the carbonyl sulfide pathway since formate intermediates are,
259 as expected, not detected (Figure 5b: no OH consumption, no formate formation). Water treatment of
260 sulfided Mo/SiO₂ has similar effect as on Mo/Al₂O₃ (Figure 5d), that is to say: almost no effect on S-
261 edge site amount and strong decrease of M-edge sites. Similarly, subsequent CO treatment creates
262 vacancy on both edges but mainly on S-edge. Meanwhile, COS and CO₂ are observed in gas phase in
263 accordance with sulfur vacancy formation. Note that contrary to Mo/Al₂O₃, the proportion of CO₂ to CO
264 formed on Mo/SiO₂ when the CO treatment is performed after the water one, is not greater than for
265 direct CO treatment just after sulfidation. This is in accordance with the absence of direct reaction
266 between SiOH and CO. Finally, resulfidation does not allow to reach back the initial sulfide site amount
267 especially on M-edge and the corresponding CO uptake of M-edge is very similar to that measured after
268 only water treatment. These results are totally in agreement with the ones obtained on Mo/Al₂O₃.

269 One difference between Mo/SiO₂ and Mo/Al₂O₃ catalysts concerns the effect of H₂O treatment on S-
270 edge sites. Indeed, even if S-edge sites are preferential sites of sulfide slabs on Mo/SiO₂, no increase in

271 S-edge sites is observed after water treatment in contrary to the case of Mo(CA=2)/Al₂O₃ (Figure 1b).
 272 This difference is related to the presence or absence of citric acid residues. As discussed in previous
 273 section, these species can react with water leading to some H₂ production and then formation of sulfur
 274 vacancies at S-edge. Hence, the involvement of carbonaceous residue proposed previously is confirmed
 275 by the absence of S-edge vacancy creation upon H₂O treatment on Mo/SiO₂.

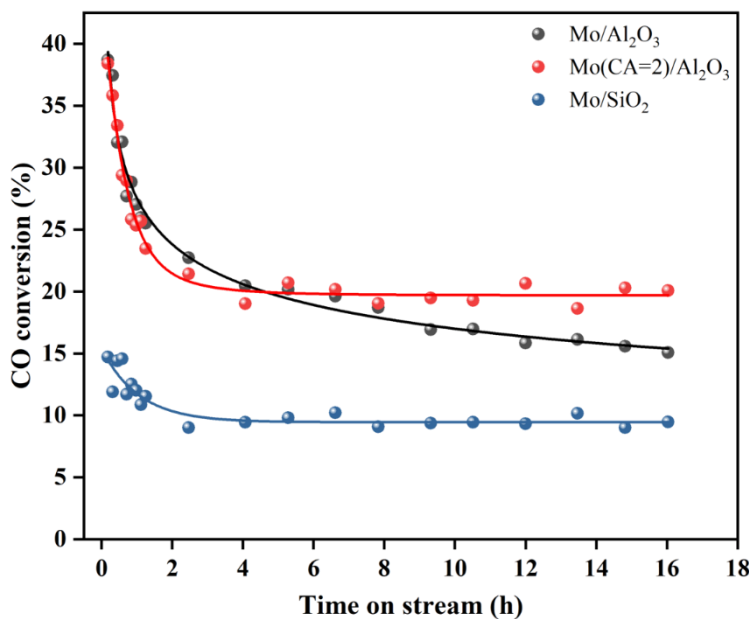


276
 277 **Figure 5. H₂O or/and CO treatment on sulfided Mo/SiO₂ catalysts.** a, CO/IR spectra of the Mo/SiO₂
 278 catalyst after sulfidation and subsequent CO treatment. b, IR spectra of Mo/SiO₂ recorded before and
 279 after CO treatment in a. c, *in situ* IR spectra of gas phase recorded during CO treatment. d, IR spectra of
 280 CO adsorption at 133 Pa equilibrium on Mo/SiO₂ catalyst after sulfidation, H₂O treatment, CO
 281 treatment and resulfidation. e, IR spectra of Mo/SiO₂ recorded before and after H₂¹⁸O treatment in d. f,
 282 *in situ* IR spectra of gas phase recorded during CO treatment on sulfided Mo/SiO₂ pretreated by H₂¹⁸O.

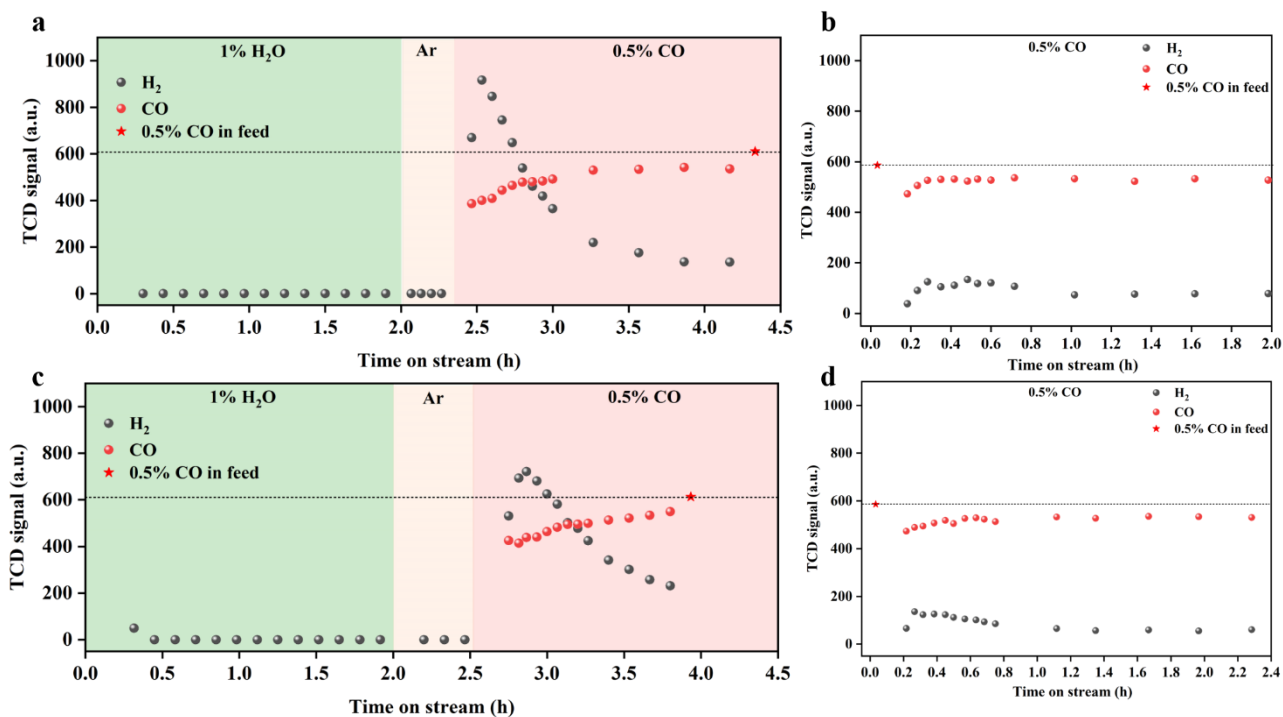
283

284 3.5. WGS activity

285 WGS performances were evaluated for Mo/Al₂O₃, Mo(CA=2)/Al₂O₃ and Mo/SiO₂ catalysts under
286 0.5% CO and 1% H₂O in Ar balance with GHSV~ 9000 h⁻¹ at 573K (Figure 6). The two alumina-
287 supported catalysts present a very strong deactivation up to 4 hours of time-on-stream (TOS). Then, the
288 activity of Mo/Al₂O₃ catalyst continues to slightly decrease while the activity of Mo(CA=2)/Al₂O₃
289 catalyst remains stable. Finally, sulfided Mo(CA=2)/Al₂O₃ catalyst exhibits a higher activity than
290 Mo/Al₂O₃ catalyst at high TOS. As for Mo/SiO₂ catalyst, it displays some deactivation up to 2 hours of
291 TOS, and then presents a stable conversion. However, the activity of Mo/SiO₂ catalyst is lower than
292 those of the alumina-supported catalysts whatever the TOS. Taking into account the complexity in terms
293 of the continuous change in M-edge site environments and the role of the interface between support and
294 sulfide sites, the intrinsic activity of the two edge sites is not possible to be determined from the initial
295 site characterization. However, the different responses of the two edges to H₂O and CO means that they
296 follow different reaction pathways.
297



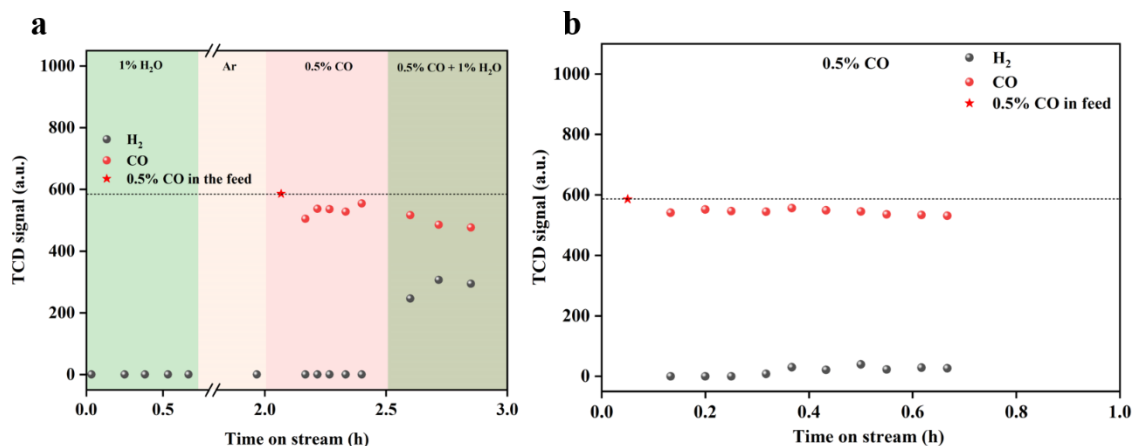
298 **Figure 6. WGS reaction vs TOS.** CO conversion over Mo/Al₂O₃, Mo(CA=2)/Al₂O₃ and Mo/SiO₂
299 catalysts during WGS reaction (feed gas: 0.5% CO and 1% H₂O in Ar balance at GHSV= 9000 h⁻¹ and
300 Tr = 573K).
301



302
 303 **Figure 7. Stepwise WGS reaction.** a, c, Water feed followed by CO feed at 573K over sulfided
 304 Mo/Al₂O₃ (a) and Mo(CA=2)/Al₂O₃ (b). b, d, CO feed at 573K on Mo/Al₂O₃ (b) and Mo(CA=2)/Al₂O₃
 305 (d).

306 Stepwise WGS reaction experiments were performed on the Al₂O₃ supported catalysts to check if the
 307 oxidation/reduction pathway was occurring (Figure 7). After sulfidation of Mo/Al₂O₃ catalyst, if only
 308 H₂O is flowing at 573 K (without CO in the flow), no H₂ signal is detected (Figure 7a). Similar behavior
 309 is observed for the sulfided Mo(CA=2)/Al₂O₃ catalyst, although a limited amount of H₂ is released at
 310 the beginning of the alone water feed (Figure 7c). As previously discussed, this small H₂ production
 311 comes from the reaction of water with residual carbonaceous species. Thus, the direct oxidation step by
 312 H₂O giving H₂ can be discarded. For both catalysts, if CO is introduced alone at 573 K after the H₂O
 313 flow, a high amount of H₂ is released and then H₂ formation reaches a much lower plateau. If now CO
 314 alone was introduced firstly after sulfidation (Figure 7b and d), a small production of H₂ occurs that is
 315 stable with TOS, and close to the plateau obtained in the previous experiment for long TOS (Figure 7a
 316 and c). Under CO alone flow, H can only come from the catalyst surface either as OH or SH species. In

317 particular, knowing that OH species can be involved in both COS hydrolysis and formate formation,
318 they can react directly (formate path) or indirectly with CO (COS path).



319

320 **Figure 8. Stepwise WGS reaction on sulfided Mo/SiO₂.** a, Water feed followed by CO feed at 573K
321 and finally followed by WGS reaction. b, CO feed at 573K.

322 Similar study was performed on Mo/SiO₂ (Figure 8). If CO is firstly introduced alone, H₂ production
323 is almost undetectable (Figure 8b). Moreover, on this catalyst, the conversion of CO and formation of
324 H₂ are not favored by the H₂O pre-treatment. As shown in Figure 8a, water in the feed is necessary to
325 produce H₂ on Mo/SiO₂. These results confirm that SiOH are not involved in the reaction pathway.

326 The WGS reaction was further studied by *operando* IR/GC experiments that combined IR analysis of
327 the surface species of the catalyst and on-line analysis by GC and gas phase IR of the reaction products
328 (Figure 9). For the three catalysts, the conversion is in the same range than in the differential reactor
329 although not totally the same. However, the same tendencies are observed as in terms of stability with
330 TOS. Indeed, alumina-supported catalysts present a marked deactivation (up to ~0.5 h) that is not
331 observed on silica-supported catalyst (Figure 9a). Moreover, alumina-supported catalyst is more stable
332 when prepared with citric acid. After stabilization, the conversion is comprised between 15 to 10% for
333 the three catalysts.

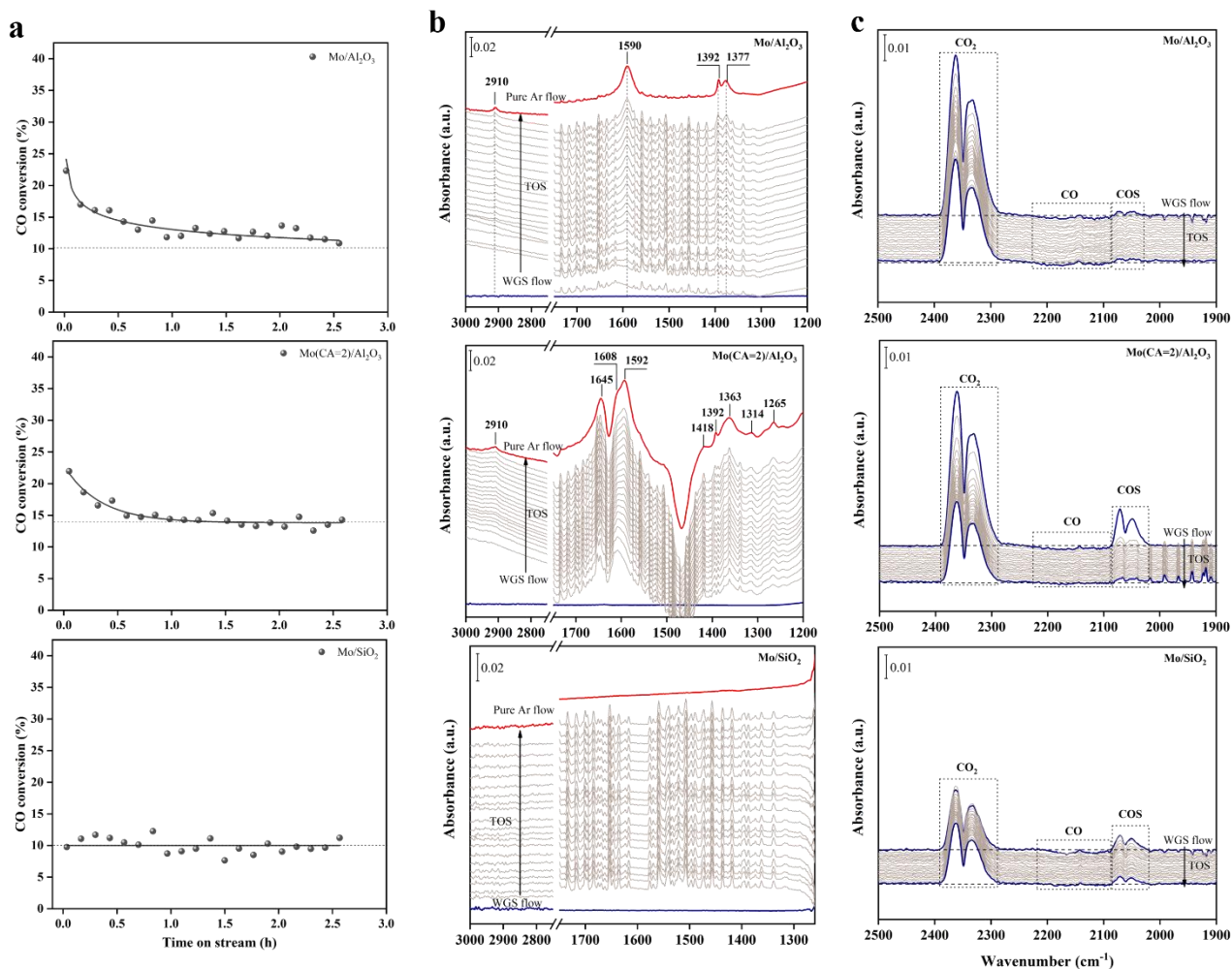
334 Meanwhile, the IR spectra of the Mo/Al₂O₃ show after a few minutes of reaction the appearance of a
335 band at 2910 cm⁻¹ as well as bands at 1590 and the doublet at 1392 and 1377 cm⁻¹ which show the
336 formation of formate species (Figure 9b). After pure Ar flow purge (red spectrum), the signal of water
337 in gas phase is eliminated which makes clearer the observation of the bands at 2910, 1590, 1392 and
338 1377 cm⁻¹. These are respectively assigned to $\nu(\text{CH})$, $\nu(\text{OCO})_{\text{asym}}$, $\delta(\text{CH})$ and $\nu(\text{OCO})_{\text{sym}}$ of formate
339 species on the Mo/Al₂O₃ catalyst surface [33]. In parallel, the gas phase IR spectra reveals CO
340 consumption and CO₂ formation as well as the formation of a limited amount of COS (Figure 9c).

341 On the IR spectra of Mo(CA=2)/Al₂O₃ catalyst, despite the presence of the complex massif due to
342 carbonaceous residues, bands characterizing formate intermediate can be observed. As with Mo/Al₂O₃,
343 CO consumption and CO₂ formation are also observed in the gas phase spectra. In addition, at the
344 beginning of the reaction, larger COS amounts are released on this catalyst than on the catalyst without
345 citric acid. However, the COS production decreases strongly and rapidly after the first TOS, and then
346 COS signal stays relatively stable and at value close to Mo/Al₂O₃.

347 On Mo/SiO₂ catalyst, no formate species are formed in agreement with the previous IR observations.
348 Meanwhile, gas phase IR spectra show CO consumption and CO₂ production as well as COS formation.
349 In this case, the COS production decreases at beginning but more slightly than for the alumina-
350 supported catalysts and then presents a stable value.

351 So in conclusion, WGS study performed in differential reactor and in the *operando* set up points out
352 that (i) activity of WGS reaction on alumina-supported catalysts is higher than that on silica-supported
353 catalyst; (ii) stability of WGS reaction decreases in the following order: Mo/SiO₂ > Mo(CA=2)/Al₂O₃ >
354 Mo/Al₂O₃ ; (iii) formate intermediates are observed only on alumina-supported catalysts ; (iv) COS
355 production occurs for all catalysts, but Mo/Al₂O₃ presents limited COS release throughout TOS; (v) for
356 Mo/SiO₂, the WGS activity should be linked only to the S-edge sites via the COS route.

357



358

359 **Figure 9. Operando IR/GC study of sulfided Mo/Al₂O₃, Mo(CA=2)/Al₂O₃ and Mo/SiO₂ during**

360 **WGS reaction at 573K versus TOS. a, CO conversion. b, IR spectra of the catalysts during the WGS**

361 **reaction (in grey) and after the reaction under Ar flow (in red) (All spectra correspond to catalyst spectra**

362 **recorded at 573 K at given TOS minus catalyst spectrum recorded at 573 K prior the WGS flow). c, IR**

363 **spectra of the gas phase during the WGS reaction (blue spectra correspond to that taken at the beginning**

364 **and at the end of the reaction. All spectra correspond to gas phase spectra recorded at given TOS minus**

365 **spectrum under the initial WGS feed flow)**

366 **3.6. New insights on WGS mechanisms on sulfide catalysts**

367 Two mechanisms are usually considered for WGS reaction over sulfide catalysts, such as the

368 associative mechanism and the redox mechanism [34]. In the associative mechanism, intermediate

369 formate species are formed on the catalyst surface via reaction of adsorbed CO with surface OH groups,
370 which then decompose to CO₂ and H₂ [21]. For the case of the redox mechanism, the surface of catalyst
371 is alternatively oxidized by water and then reduced by CO[12, 13].

372 Based (i) on the results of stepwise reactions and in particular on the production of H₂ under the CO
373 alone feed, (ii) from the direct observation of formate intermediates in *operando* studies and (iii) the
374 observed decomposition of formate at 573K on Mo/Al₂O₃, one can conclude that the formate
375 mechanism occurs on Al₂O₃-supported MoS₂ catalysts at 573K. It must be underlined that at this
376 temperature, WGS reaction does not occur on pure alumina, indicating that the vicinity between the Al-
377 OH groups and the sulfide phase facilitates the formate species formation and thus play a role in the
378 catalyst reactivity.

379 However, various observations point out that another reaction route exists. Indeed, silica-supported
380 MoS₂ catalyst present a stable CO conversion whereas no formate species are formed during the WGS
381 reaction. The conventional redox mechanism was firstly considered, in which the water-induced
382 Mo(S_xO_y)_{zc} site is proposed as the active center and then reduced by CO to produce CO₂ and give rise to
383 a vacancy site [12, 13]. However, the CO/IR studies (Figure 4) vividly demonstrate that this oxygen
384 substituted Mo(S_xO_y)_{zc} site formed in situ by water treatment is stable toward CO treatment, thus
385 preventing a direct redox process. In addition, this Mo(S_xO_y)_{zc} site also shows excellent stability even in
386 10% H₂S/H₂ treatment and thus cannot be re-sulfided back to the initial state. These results suggest that
387 the proposition of the conventional redox mechanism associated with Mo(S_xO_y)_{zc} site might not be
388 correct, and this water-induced S/O exchange reaction is an irreversible poisoning process for MoS₂,
389 especially for M-edge site.

390 The IR gas phase spectra collected during the WGS reaction substantiate the formation of COS
391 production. Thus, a novel redox mechanism associated with COS route can be proposed (equation 1-3).
392 In this three-stage novel mechanism, the catalyst surface is firstly reduced by CO to form COS, then

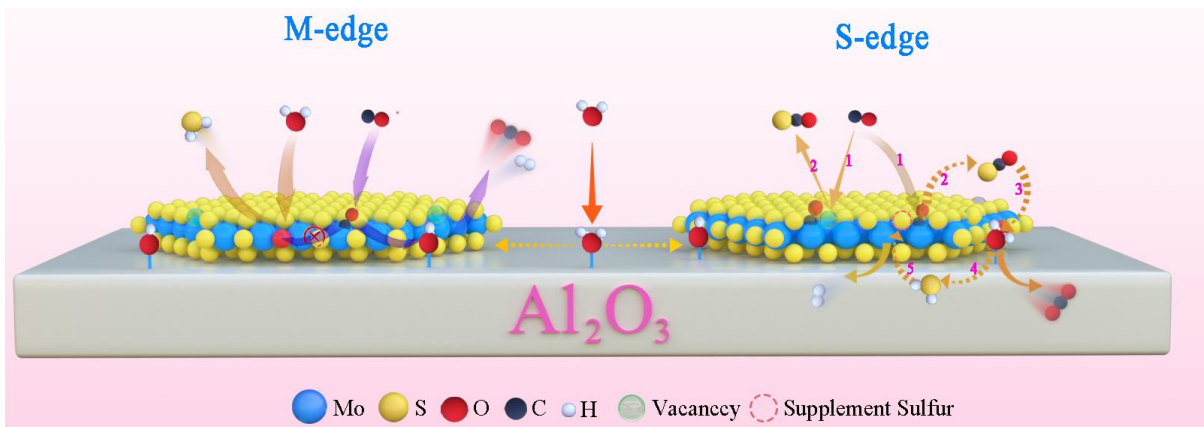
393 COS is hydrolyzed to give rise to CO₂ and H₂S, and finally the sulfur vacancy can be refilled by H₂S to
394 returns back to its pre-reaction surface state:



398 This proposal is consistent with both γ -Al₂O₃ and sulfide phase known as commercial COS hydrolysis
399 catalysts [35, 36], and MoS₂ catalyst recognized as a good candidate for H₂S decomposition to yield H₂
400 [37]. In addition, under the regime of the COS hydrolysis pathway during WGS reaction, the
401 unconverted COS inevitably leads to sulfur loss, which also well explains why addition of H₂S in the
402 feed leads to a high and stable catalytic performance [5, 22].

403 Interestingly, Table 1 shows that CO forms vacancies on S-edge, and not on M-edge. Hence, this
404 novel redox mechanism involving COS can be exclusively ascribed to the S-edge sites. Note that one
405 cannot exclude that the formate route may also happen on the S-edge of alumina-supported catalysts. On
406 contrary, the activity of M-edge sites in WGS is only ascribed to the formate mechanism. Consequently,
407 on Mo/SiO₂, these M-edge sites should not be involved in reaction and CO conversion is entirely due to
408 the contribution of the COS pathway at S-edge. Knowing that the M-edge sites are irreversibly sensitive
409 to water, the deactivation with TOS observed on Al₂O₃ supported catalysts and more strongly on
410 Mo/Al₂O₃ having lower S/M edge ratio (Figure 6) can then be ascribed to these M-edge sites.

411 Hence, on Al₂O₃-supported MoS₂ catalysts, both formate and COS redox reaction routes occur
412 preferentially on M- and S-edge sites, respectively (Figure 10). As a general conclusion, the nature of
413 the support and the S-/M-edge ratio of the sulfide slabs determine the mechanisms and the stability of
414 the WGS reaction.



415

416 **Figure 10:** Schematic of reaction routes for WGS reaction over M-edge and S-edge sites of MoS₂ slab.

417 4. Conclusion

418 The effects of WGS reactants (H₂O, CO) on M-edge and the S-edge sites of MoS₂ catalysts were
 419 explored by *in situ* IR spectroscopy. IR/CO experiments demonstrated that the M-edge site is sensitive
 420 to water to form the oxygen-substituted Mo(S_xO_y)_{zc} site via S/O exchange reaction, while the S-edge
 421 site is sensitive to CO to form vacancies and release COS. Stepwise reaction experiments and IR
 422 Operando study revealed that two different WGS pathways are involved in H₂ production on sulfide: (i)
 423 Hydrogen can be produced by WGS reaction following formate mechanism i.e. through the reaction of
 424 CO with hydroxyl group of alumina support; (ii) Hydrogen can also be produced by a redox mechanism.
 425 However, the conventional redox mechanism that occurs by direct oxidation by water and subsequent
 426 reduction by CO has to be excluded on the Mo-sulfide catalysts. Moreover, the stability of Mo(S_xO_y)_{zc}
 427 species towards CO exclude their role as WGS active centers. However, the detection of COS formation
 428 during WGS reaction leads to propose a novel redox mechanism associated with this intermediate.
 429 Interestingly, the findings in different response of two edge site towards CO indicate that formate route
 430 occurs mainly on the M-edge, while the novel redox mechanism occurs exclusively on S-edge of the
 431 sulfide slabs. Finally, WGS tests show that the M-edge site is not a stable and durable active center
 432 compared with S-edge.

433 This work gives the direction for obtaining high stability sulfide catalyst for reactions involving water
 434 by improving stability of M-edge sites and also reveals that the active sites of CO activation and

435 oxidation are located at the S-edge, which also contributes to the design of sulfide catalysts for other
436 reaction, such as methanethiol synthesis.
437

Corresponding Author: * E-mail: laetitia.oliviero@ensicaen.fr

ORCID: Laetitia Oliviero: <https://orcid.org/0000-0002-7931-439X>

Author Contributions

The manuscript was written through contributions of all authors. All authors have given approval to the final version of the manuscript.

Funding Sources

W. Zhao is grateful for the MOPGA grant (Campus France MOPGA-927541K)

Acknowledgments

Alexandre Vimont, Philippe Bazin and Yoann Levaque from LCS are greatly acknowledged for the IR experiments and activity measurements for WGS reaction. The authors thank Jinxing Mi and Xiaoping Chen for kindly helping with Graphical abstract and Scheme design.

REFERENCES

- [1] J. Kibsgaard, Z. Chen, B.N. Reinecke, T.F. Jaramillo, Engineering the surface structure of MoS₂ to preferentially expose active edge sites for electrocatalysis, *Nat Mater*, 11 (2012) 963-969.
- [2] L. Liu, J. Wu, L. Wu, M. Ye, X. Liu, Q. Wang, S. Hou, P. Lu, L. Sun, J. Zheng, L. Xing, L. Gu, X. Jiang, L. Xie, L. Jiao, Phase-selective synthesis of 1T' MoS₂ monolayers and heterophase bilayers, *Nat Mater*, 17 (2018) 1108-1114.
- [3] J. Hu, L. Yu, J. Deng, Y. Wang, K. Cheng, C. Ma, Q. Zhang, W. Wen, S. Yu, Y. Pan, J. Yang, H. Ma, F. Qi, Y. Wang, Y. Zheng, M. Chen, R. Huang, S. Zhang, Z. Zhao, J. Mao, X. Meng, Q. Ji, G.

- Hou, X. Han, X. Bao, Y. Wang, D. Deng, Sulfur vacancy-rich MoS₂ as a catalyst for the hydrogenation of CO₂ to methanol, *Nature Catalysis*, 4 (2021) 242-250.
- [4] J. Chen, F. Maugé, J. El Fallah, L. Oliviero, IR spectroscopy evidence of MoS₂ morphology change by citric acid addition on MoS₂/Al₂O₃ catalysts – A step forward to differentiate the reactivity of M-edge and S-edge, *J. Catal.*, 320 (2014) 170-179.
- [5] T. Sasaki, T. Suzuki, H. Iizuka, M. Takaoka, Reaction mechanism analysis for molybdenum-based water-gas shift catalysts, *Applied Catalysis A: General*, 532 (2017) 105-110.
- [6] B. Hinnemann, P.G. Moses, J. Bonde, K.P. Jorgensen, J.H. Nielsen, S. Horch, I. Chorkendorff, J.K. Nørskov, Biomimetic hydrogen evolution: MoS₂ nanoparticles as catalyst for hydrogen evolution, *J. Am. Chem. Soc.*, 127 (2005) 5308-5309.
- [7] T.F. Jaramillo, K.P. Jorgensen, J. Bonde, J.H. Nielsen, S. Horch, I. Chorkendorff, Identification of active edge sites for electrochemical H₂ evolution from MoS₂ nanocatalysts, *Science*, 317 (2007) 100-102.
- [8] J. Peto, T. Ollar, P. Vancso, Z.I. Popov, G.Z. Magda, G. Dobrik, C. Hwang, P.B. Sorokin, L. Tapaszto, Spontaneous doping of the basal plane of MoS₂ single layers through oxygen substitution under ambient conditions, *Nat Chem*, 10 (2018) 1246-1251.
- [9] Z. Wang, Q. Li, H. Xu, C. Dahl-Petersen, Q. Yang, D. Cheng, D. Cao, F. Besenbacher, J.V. Lauritsen, S. Helveg, M. Dong, Controllable etching of MoS₂ basal planes for enhanced hydrogen evolution through the formation of active edge sites, *Nano Energy*, 49 (2018) 634-643.
- [10] S.S. Grønberg, K. Thorarinsdóttir, L. Kyhl, J. Rodríguez-Fernández, C.E. Sanders, M. Bianchi, P. Hofmann, J.A. Miwa, S. Ulstrup, J.V. Lauritsen, Basal plane oxygen exchange of epitaxial MoS₂ without edge oxidation, *2D Materials*, 6 (2019).
- [11] J. Xie, J. Zhang, S. Li, F. Grote, X. Zhang, H. Zhang, R. Wang, Y. Lei, B. Pan, Y. Xie, Controllable disorder engineering in oxygen-incorporated MoS₂ ultrathin nanosheets for efficient hydrogen evolution, *J. Am. Chem. Soc.*, 135 (2013) 17881-17888.
- [12] P. Hou, D. Meeker, H. Wise, Kinetic studies with a sulfur-tolerant water gas shift catalyst, *J. Catal.*, 80 (1983) 280-285.
- [13] C.R.F. Lund, Microkinetics of Water–Gas Shift over Sulfided Mo/Al₂O₃ Catalysts, *Industrial & Engineering Chemistry Research*, 35 (1996) 2531-2538.
- [14] H. Schweiger, P. Raybaud, G. Kresse, H. Toulhoat, Shape and Edge Sites Modifications of MoS₂ Catalytic Nanoparticles Induced by Working Conditions: A Theoretical Study, *J. Catal.*, 207 (2002) 76-87.

- [15] J. Lauritsen, J. Kibsgaard, G. Olesen, P. Moses, B. Hinnemann, S. Helveg, J. Nørskov, B. Clausen, H. Topsøe, E. Lægsgaard, Location and coordination of promoter atoms in Co- and Ni-promoted MoS₂-based hydrotreating catalysts, *J. Catal.*, 249 (2007) 220-233.
- [16] J.V. Lauritsen, M.V. Bollinger, E. Lægsgaard, K.W. Jacobsen, J.K. Nørskov, B.S. Clausen, H. Topsøe, F. Besenbacher, Atomic-scale insight into structure and morphology changes of MoS₂ nanoclusters in hydrotreating catalysts, *J. Catal.*, 221 (2004) 510-522.
- [17] A.S. Walton, J.V. Lauritsen, H. Topsøe, F. Besenbacher, MoS₂ nanoparticle morphologies in hydrodesulfurization catalysis studied by scanning tunneling microscopy, *J. Catal.*, 308 (2013) 306-318.
- [18] J. Bonde, P.G. Moses, T.F. Jaramillo, J.K. Nørskov, I. Chorkendorff, Hydrogen evolution on nanoparticulate transition metal sulfides, *Faraday Discuss.*, 140 (2008) 219-231; discussion 297-317.
- [19] Y.-Y. Chen, M. Dong, J. Wang, H. Jiao, On the Role of a Cobalt Promoter in a Water-Gas-Shift Reaction on Co-MoS₂, *The Journal of Physical Chemistry C*, 114 (2010) 16669-16676.
- [20] Y.-Y. Chen, M. Dong, J. Wang, H. Jiao, Mechanisms and Energies of Water Gas Shift Reaction on Fe-, Co-, and Ni-Promoted MoS₂ Catalysts, *The Journal of Physical Chemistry C*, 116 (2012) 25368-25375.
- [21] C. Zhang, B. Liu, L. Zhao, Q. Zong, J. Gao, Y. Wang, C. Xu, Insights into water-gas shift reaction mechanisms over MoS₂ and Co-MoS₂ catalysts: a density functional study, *Reaction Kinetics, Mechanisms and Catalysis*, 120 (2017) 833-844.
- [22] S. Yun, V.V. Gulians, Support Effects on Water Gas Shift Activity and Sulfur Dependence of Mo Sulfide Catalysts, *Energy & Fuels*, 33 (2019) 11655-11662.
- [23] C. Hulteberg, Sulphur-tolerant catalysts in small-scale hydrogen production, a review, *Int. J. Hydrogen Energy*, 37 (2012) 3978-3992.
- [24] J.A. Singh, S.H. Overbury, N.J. Dudney, M. Li, G.M. Veith, Gold Nanoparticles Supported on Carbon Nitride: Influence of Surface Hydroxyls on Low Temperature Carbon Monoxide Oxidation, *ACS Catalysis*, 2 (2012) 1138-1146.
- [25] D. Lorito, A. Paredes-Nunez, C. Mirodatos, Y. Schuurman, F.C. Meunier, Determination of formate decomposition rates and relation to product formation during CO hydrogenation over supported cobalt, *Catal. Today*, 259 (2016) 192-196.
- [26] E. Dominguez Garcia, J. Chen, E. Oliviero, L. Oliviero, F. Maugé, New insight into the support effect on HDS catalysts: evidence for the role of Mo-support interaction on the MoS₂ slab morphology, *Applied Catalysis B: Environmental*, 260 (2020).

- [27] J. Chen, E. Dominguez Garcia, L. Oliviero, F. Maugé, How the CO molar extinction coefficient influences the quantification of active sites from CO adsorption followed by IR spectroscopy? A case study on MoS₂/Al₂O₃ catalysts prepared with citric acid, *J. Catal.*, 332 (2015) 77-82.
- [28] A. Travert, C. Dujardin, F. Maugé, S. Cristol, J.F. Paul, E. Payen, D. Bougeard, Parallel between infrared characterisation and ab initio calculations of CO adsorption on sulphided Mo catalysts, *Catal. Today*, 70 (2001) 255-269.
- [29] D. Mey, S. Brunet, C. Canaff, F. Maugé, C. Bouchy, F. Diehl, HDS of a model FCC gasoline over a sulfided CoMo/Al₂O₃ catalyst: Effect of the addition of potassium, *J. Catal.*, 227 (2004) 436-447.
- [30] W. Chen, F. Maugé, J. van Gestel, H. Nie, D. Li, X. Long, Effect of modification of the alumina acidity on the properties of supported Mo and CoMo sulfide catalysts, *J. Catal.*, 304 (2013) 47-62.
- [31] L. Zavala-Sanchez, X. Portier, F. Mauge, L. Oliviero, High-resolution STEM-HAADF microscopy on a gamma-Al₂O₃ supported MoS₂ catalyst-proof of the changes in dispersion and morphology of the slabs with the addition of citric acid, *Nanotechnology*, 31 (2020) 035706.
- [32] M. Badawi, J.F. Paul, S. Cristol, E. Payen, Y. Romero, F. Richard, S. Brunet, D. Lambert, X. Portier, A. Popov, E. Kondratieva, J.M. Goupil, J. El Fallah, J.P. Gilson, L. Mariey, A. Travert, F. Maugé, Effect of water on the stability of Mo and CoMo hydrodeoxygenation catalysts: A combined experimental and DFT study, *J. Catal.*, 282 (2011) 155-164.
- [33] N.C. Nelson, M.-T. Nguyen, V.-A. Glezakou, R. Rousseau, J. Szanyi, Carboxyl intermediate formation via an in situ-generated metastable active site during water-gas shift catalysis, *Nature Catalysis*, 2 (2019) 916-924.
- [34] R.A. Ojifinni, N.S. Froemming, J. Gong, M. Pan, T.S. Kim, J.M. White, G. Henkelman, C.B. Mullins, Water-enhanced low-temperature CO oxidation and isotope effects on atomic oxygen-covered Au(111), *J. Am. Chem. Soc.*, 130 (2008) 6801-6812.
- [35] C. Rhodes, S.A. Riddel, J. West, B.P. Williams, G.J. Hutchings, The low-temperature hydrolysis of carbonyl sulfide and carbon disulfide: a review, *Catal. Today*, 59 (2000) 443-464.
- [36] Z. George, Kinetics of cobalt-molybdate-catalyzed reactions of SO₂ with H₂S and COS and the hydrolysis of COS*1, *J. Catal.*, 32 (1974) 261-271.
- [37] L. Sharma, R. Upadhyay, S. Rangarajan, J. Baltrusaitis, Inhibitor, Co-Catalyst, or Co-Reactant? Probing the Different Roles of H₂S during CO₂ Hydrogenation on the MoS₂ Catalyst, *ACS Catalysis*, 9 (2019) 10044-10059.

Supporting Information. IR study of MoS₂/Al₂O₃ catalysts prepared with and without citric acid (CA)
- Effect of H₂ treatment on sulfided Mo(CA=2)/Al₂O₃ - In-situ IR spectra during H₂¹⁸O treatment on sulfided Mo(CA=2)/Al₂O₃ - Effect of resulfidation - Formation of formate species on Mo/Al₂O₃ upon CO treatment - Decomposition of formate species on Mo/ Al₂O₃ - Post-treatment followed by CO/IR characterization - Spectra treatment and concentration of sites calculation.
